Available at www.sciencedirect.com

ScienceDirect

journal homepage: www.elsevier.com/locate/he

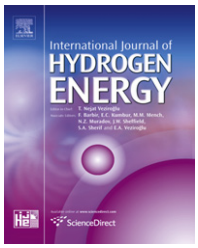

Impedance and hydrogen evolution studies on magnesium alloy in oxalic acid solution containing different anions

A.M. Fekry

Chemistry Department, Faculty of Science, Cairo University, Giza 12613, Egypt

ARTICLE INFO

Article history:
Received 9 July 2010
Received in revised form
11 August 2010
Accepted 21 August 2010

Keywords:
AZ31E alloy
Oxalic acid
EIS
Polarization
SEM

ABSTRACT

The corrosion behavior of AZ31E alloy was investigated in oxalic acid solution using different electrochemical techniques. The effect of concentration was studied, where the corrosion rate was found to increase with increasing oxalic acid concentration and hydrogen evolution. The effect of adding Cl^-, F^- or PO_4^{3-} ions on the electrochemical behavior of AZ31E electrode was studied in 0.01 M oxalic acid solution at 298 K. It was found that the corrosion rate increases with increasing Cl^- or F^- ion concentration, however, it decreases with increasing PO_4^{3-} ion concentration. Good agreement was observed between the results obtained from electrochemical techniques and confirmed by Scanning electron micrographs.

1. Introduction

Magnesium is the lightest of all metals in practical use, and has a density (1.74D g cm^{-3}) of about two thirds of aluminum [1]. Magnesium alloys have many unique properties compared with other metals. Their most attractive feature is their very high strength-to-weight ratio. Magnesium can form intermetallic phases with most of the alloying elements. The stability of this phase increases with the increasing electronegativity of the other added element [2]. Aluminum (Al) had already become the most important alloying element for significantly increasing the tensile strength, specifically by forming the intermetallic phase $Mg_{17}Al_{12}$. Similar effects can be achieved with zinc (Zn) and manganese (Mn) [3]. The AZ-based Mg system has been the basis of the most widely used magnesium alloys. Among these alloys, AZ31E is the most successful alloy having excellent mechanical properties. Nevertheless, a serious limitation for the wide-spread use of several magnesium alloys is their susceptibility to general and localized (pitting) corrosion. Extruded Mg alloys as AZ31E is getting more and more widely used because of their considerably high plasticity in comparison with the die-cast Mg alloys [4]. This makes studying the corrosion and corrosion control of Mg alloys an interesting point of research which can enable extending the potential use of these important materials in a broad range of many technical and innovative applications.

Oxalic acid is a relatively strong organic acid used as purifying agent in pharmaceutical industry [5]. Oxalic acid's main applications include cleaning or bleaching, especially for the removal of rust. The charge on oxalic acid allows it to act as a chelator of various positively charged metal ions [6]. The present work aims to attain more information concerning the hydrogen evolution rate and corrosion behavior of AZ31E Mg-based alloy in oxalic acid solution containing Cl^-, F^- or PO_4^{3-} anions under various environmental conditions. Different techniques were employed such as open circuit potential (OCP), potentiodynamic polarization, impedance spectroscopy (EIS) and scanning electron microscope (SEM) technique.

E-mail address: hham4@hotmail.com.
0360-3199/$ – see front matter © 2010 Professor T. Nejat Veziroglu. Published by Elsevier Ltd. All rights reserved.
doi:10.1016/j.ijhydene.2010.08.116

2. Experimental

A Sample of extruded AZ31 alloy was donated from GMN, Laval University, Canada with chemical composition (wt%) as given in Table 1. The sample was divided into small coupons. Each coupon was welded to an electrical wire and fixed with Araldite epoxy resin in a glass tube leaving cross-sectional area of 0.196 cm^2 for the tested sample. The surface of the test electrode was mechanically polished by emery papers with 400 up to 1000 grit to ensure the same surface roughness, degreasing in acetone, rinsing with ethanol and drying in air. The cell used was a typical three-electrode one fitted with a large platinum sheet of size 15 × 20 × 2 mm as a counter electrode (CE), saturated calomel (SCE) as a reference electrode (RE) and AZ31E alloy as the working electrode (WE) [4]. The solutions were prepared using Analar grade reagents (oxalic acid, sodium fluoride, sodium chloride and sodium phosphate) and triply distilled water.

The instrument used is the electrochemical workstation IM6e Zahner-elektrik, GmbH, (Kronach, Germany). Cathodic and anodic polarization curves were scanned from −2.0 V to −1.0 V with a scan rate of 1 mV s^{-1}. The impedance diagrams were recorded at the free immersion potential (OCP) by applying a 10 mV sinusoidal potential through a frequency domain from 100 kHz down to 100 mHz. All potentials were measured and given with respect to SCE (E = 0.241 V). The electrochemical experiments were always carried out inside an air thermostat keep at 25 °C. The SEM micrographs were collected using a JEOL JXA-840A electron probe microanalyzer.

3. Results and discussion

3.1. Open circuit measurements

The open circuit potential (E_{oc}) of AZ31E electrode was followed over a period of 2 h in naturally aerated oxalic acid solution of different concentrations including (0.01, 0.25, 0.5 and 1.0 M) and referred relative to a saturated calomel electrode. It was found that final electrode potential (E_f) shifts negatively with increasing acid concentration as shown in Fig. 1. This indicates dissolution of the surface film [5] which is due to increasing hydrogen evolution in the medium and decreasing pH. Also, E_f of AZ31E alloy was measured in 0.01 M oxalic acid containing different anions including Cl^-, F^- and PO_4^{3-} with different concentrations ranging from 0.01 to 1.0 M at 298 K. The results were illustrated in Fig. 1. The way in which a metal or an alloy changes its potential upon immersion in solution indicates the nature of the reaction taking place at the surface. In 0.01 M oxalic acid solution containing Cl^- or F^- ion, E_f tends to more negative values with increasing their concentration. This is due to their aggressiveness, which

Table 1 – Chemical analysis in wt % of AZ31E alloy.

Material	Al	Zn	Mn	Cu	Fe	Ni	Be	Balance
AZ31E	2.8	0.96	0.28	0.0017	0.0111	0.0007	0.0001	Mg

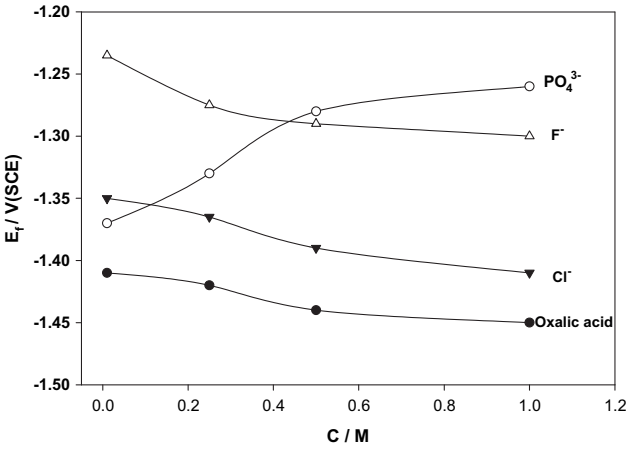

Fig. 1 – Variation of final steady state potential (E_f) of AZ31E electrode as a function of concentration for oxalic acid and Cl^-, F^- or PO_4^{3-} anions in naturally aerated 0.01 M oxalic acid solution, at 298 K.

means that increasing their concentration deteriorate the passive film formed on the electrode surface. Same results was obtained previously [5] for titanium alloy in oxalic acid solution containing chloride ion. The adsorbed anions as chloride or fluoride can form soluble magnesium halide (MgX_2), being higher for $MgCl_2$ [7] and lower for MgF_2, on the alloy surface.

On the other hand phosphate has an opposite effect, where increasing its concentration shifts E_f to more positive values. This means that increasing of phosphate concentration improves the passivity of the film. The results in general indicate that phosphate ion when reacted with oxalic acid as chelating agent forming phosphate complexes that sustains the process of oxide film formation as a result of spontaneous oxidation of the surface with the increasing phosphate concentration [1]. Also, increasing phosphate concentration leads to an increase in the pH of the medium and a decrease in hydrogen evolution.

3.2. EIS measurements

The impedance diagrams were recorded at the free immersion potential (OCP) by applying a 10 mV sinusoidal potential through a frequency domain from 100 kHz down to 100 mHz. The impedance measurements recorded after 2 h of immersion for AZ31E electrode in oxalic acid solution with different concentrations are presented in Fig. 2. Bode plots show an intermediate frequency phase peak shifts to lower frequency and higher phase angle maximum with decreasing oxalic acid concentration. Also, impedance values increase with decreasing the concentration of oxalic acid. The appropriate equivalent model used (Fig. 3) consists of two circuits in series from $R_1C_1Z_W$ and R_2C_2 parallel combination and both are in series with R_s. C_1 is related to capacitance of the outer layer and faradaic reaction therein, C_2 pertains to the inner layer, while R_1 and R_2 are the respective resistances of the outer and inner layers constituting the surface film, respectively [8]. Warburg impedance (Z_W) was introduced to account for the

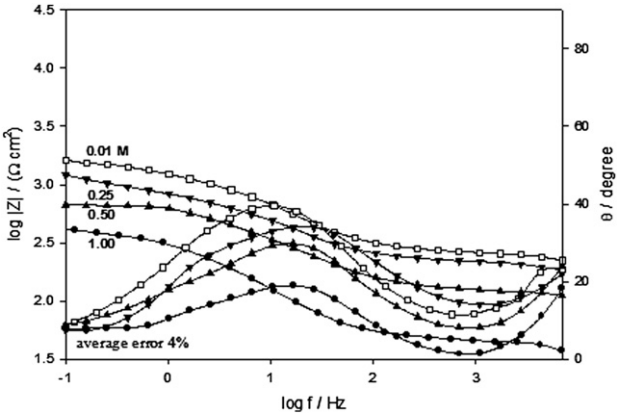

Fig. 2 – Bode plots of AZ31E electrode in naturally aerated oxalic acid solution of different concentrations, at 298 K.

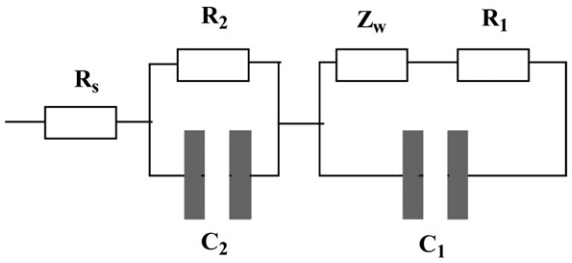

Fig. 3 – Equivalent circuit used to fit the experimental impedance data.

presence of a diffusion process within the outer layer. In all cases, good conformity between theoretical and experimental results was obtained with an average error of 4%. The evaluated experimental values are given in Table 2.

It was found that, when AZ31E electrode was immersed in oxalic acid solution, two competitive processes occur. The first one is oxide formation which yields a compact magnesium oxide film with good corrosion resistance. The second one is the formation of magnesium oxalate complexes, which yields a thick porous film as in case of Aluminum alloys [9] with expected low corrosion resistance, where oxalate ions are bidentate ligands capable of forming strong surface complexes. With increasing of oxalic acid concentration the alternation of the compact oxide film by porous oxalate one will increase by leading consequently to the increasing of corrosion rate. This also is due to increasing of the acidity of the medium that leads to increasing the hydrogen production. This leads to increasing hydrogen evolution in the medium and increasing corrosion rate.

In Table 2, R_1 represents the resistance of the passive film which decreases with increasing of oxalic acid concentration due to alternation of compact film by porous one. Consequently, the decrease in the relative thickness of the passive film ($1/C_1$) supports this concept. As the most stable formula for magnesium oxalate is dehydrated one [3], so R_2 can represent the resistance of the hydrated layer and the decreasing of relative thickness ($1/C_2$) of this layer with increasing of oxalic acid concentration reflects the strong adsorption of the oxalate anion with increasing of its concentration and increasing of hydrogen evolution. Moreover, the presence of diffusion process at the interfacial layer of the electrode indicates again the formation of porous film and the decreasing of diffusion impedance indicating the increase of electrolyte diffusion through the pores, as a sequence of increasing of the porosity with the increase of oxalate concentration.

At the lowest concentration of oxalic acid (0.01 M) with highest corrosion resistance, the tested electrode was immersed in this solution containing either Cl^-, F^- or PO_4^{3-} ions with various anion concentrations (0.01–1.0 M). After reaching steady state potential values, measurements of the impedance were done and shown in Figs. 4 and 5 as examples for Cl^- and PO_4^{3-} ions, respectively. The EIS results of the tested electrode were analyzed, following the suitable proposed model for the metal film system shown in Fig. 3. The theoretical simulated parameters for the tested alloy at each concentration from the added anions (Cl^-, F^- or PO_4^{3-}) to the forming 0.01 M oxalic acid solution were computed and summarized in Table 3.

In chloride or fluoride additive solutions, the total resistance (Fig. 6), Warburg resistance and the relative thickness (1/C) decreases with increasing its concentrations. As stated previously, this is due to the deleterious effect of chloride ions [5]. For F^- ions, in the formation of MgF_2, an oxidation reaction occurred as follows:

$$Mg + 2H_2O \rightarrow Mg(OH)_2 + H_2\uparrow \quad (1)$$

Since $Mg(OH)_2$ was not stable in acidic solution [10], reactions should occur as follows:

$$Mg(OH)_2 + 2HF \rightarrow MgF_2 + 2H_2O \quad (2)$$

$$Mg(OH)_2 \rightarrow MgO + H_2O \quad (3)$$

The overall reaction occurred as follows:

$$Mg + H_2O + 2F^- \rightarrow MgO + MgF_2 + H_2\uparrow \quad (4)$$

Table 2 – Impedance parameters of AZ31E electrode in naturally aerated oxalic acid of different concentrations, at 298 K.

$Na_2C_2O_4$	R_1	C_1	α_1	R_2	W	C_2	α_2	R_s
M	kΩ cm²	μF cm⁻²		Ω cm²	kDW	μF cm⁻²		Ω cm²
0.01	2.1	4.7	0.94	58.3	10.2	19.2	0.58	243
0.25	1.3	5.4	0.93	35.6	9.7	20.1	0.56	200
0.50	0.8	6.6	0.91	22.3	7.5	21.3	0.55	100
1.00	0.7	8.3	0.90	14.4	5.2	22.0	0.52	44

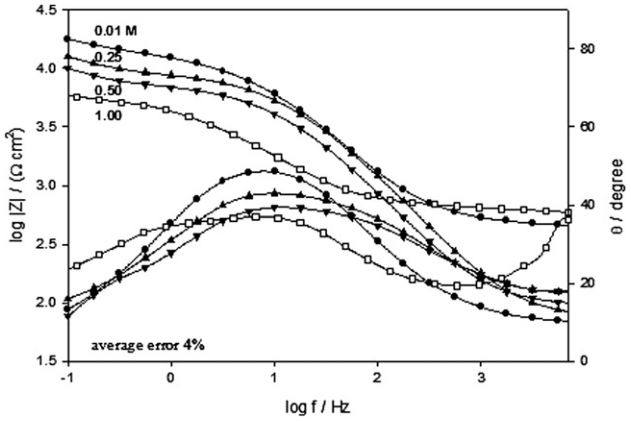

Fig. 4 – Bode plots of AZ31E electrode as a function of concentration for Cl^- anion in naturally aerated 0.01 M oxalic acid solution, at 298 K.

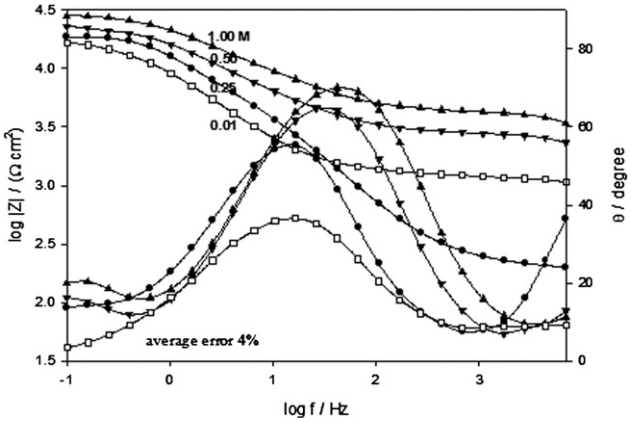

Fig. 5 – Bode plots of AZ31E electrode as a function of concentration for PO_4^{3-} anion in naturally aerated 0.01 M oxalic acid solution, at 298 K.

The pores in the film should be generated by the evolution of hydrogen. These pores might be decreased or filled by the precipitation of MgF_2 particles [10], thus presence of fluoride decreases the corrosion of tested alloy than the blank (0.01 M oxalic acid). However, depassivation process occurs by increasing fluoride concentration due to breakdown of formed grained layer of MgF_2. This will lead to drastic increase in the surface roughness. Furthermore, in presence of F^- ions, aluminum which becomes enriched in the surface can form the soluble complex $(AlF_6)^{3-}$, thereby, participates at higher F^- ions concentrations in decreasing the stability of the passive surface film on AZ31E alloy [7]. However, Cl^- ion is more strongly adsorbed on the alloy surface than F^- ions, so, its resistivity is lower than fluoride ion.

In phosphate additive anion, increasing of total resistance (R_T) (Fig. 6), W and relative thickness ($1/C_1$) with increasing of phosphate concentration indicates that interaction between oxalic acid and phosphate forms phosphate complexes that increase with increasing phosphate concentration and leads to passivation of AZ31E surface. Also, by measuring the pH of the medium, it increases slightly from acidic ~ 6.8 to basic medium reaching to 11.1 at 1.0 M phosphate concentration, leading to passivation. It is obvious that at pH 11.1, HPO_4^{2-} species has almost equal tendency for existing in solution as PO_4^{3-} anions and thus the solution at this pH will contain the two phosphate species with nearly equal relative fraction [1,11,12]. Therein the electrolyte pH plays a determinant influence on film properties, where films formed in phosphate solutions at higher pH values are thicker of better protection for the alloy than those formed in acidic ones. Also hydrogen evolution rate decreases with the increase in pH value.

General conclusion from these series of experiments is that in albeit of the classification of these anions according to their corrosiveness is different, where Cl^- and F^- ions are corrosive and PO_4^{3-} anion is passivator [7], all these anions were corrosive when they interact with oxalate anion.

Impedance results were confirmed by scanning electron micrographs shown in Fig. 7, where Fig. 7a is for the blank which is corroded without a clear film formed on the surface, after addition of 0.01 M of PO_4^{3-} (Fig. 7b), a compact film of

Table 3 – Impedance and corrosion parameters of AZ31E electrode as a function of concentration for Cl^-, F^- and PO_4^{3-} anions in naturally aerated 0.01 M oxalic acid, at 298 K.

Anion	C	R_1	C_1	α_1	R_2	W	C_2	α_2	R_s	i_{corr}
	M	KΩ cm²	μF cm⁻²		Ω cm²	kDW	nF cm⁻²		Ω cm²	μA cm⁻²
Cl^-	blank	2.10	4.7	0.84	58.3	10.2	19.2	0.58	243	31.7
	0.01	20.0	2.5	0.83	94.1	5.30	7.60	0.57	501	13.4
	0.25	14.3	2.9	0.83	87.4	4.30	11.9	0.56	80	16.7
	0.50	10.5	3.9	0.81	82.1	3.10	14.9	0.54	100	20.6
	1.00	6.70	4.1	0.84	63.7	1.50	18.6	0.53	589	25.1
F^-	blank	2.10	4.7	0.84	58.3	10.2	19.2	0.58	243	31.7
	0.01	23.8	2.1	0.81	110	9.30	5.30	0.59	208	10.8
	0.25	21.3	2.5	0.87	106	8.60	6.40	0.67	80	11.2
	0.50	18.6	2.6	0.87	91.6	7.50	9.60	0.62	100	12.1
	1.00	15.8	2.8	0.81	69.2	6.70	10.1	0.59	589	14.0
PO_4^{3-}	blank	2.10	4.7	0.84	58.3	10.2	19.2	0.58	243	31.7
	0.01	17.0	2.4	0.87	121	4.20	7.40	0.57	1075	30.0
	0.25	20.1	2.1	0.88	143	5.40	6.10	0.52	199	15.8
	0.50	24.2	1.2	0.85	165	6.20	5.60	0.56	2290	3.50
	1.00	28.9	0.6	0.82	198	8.10	4.70	0.65	3388	2.41

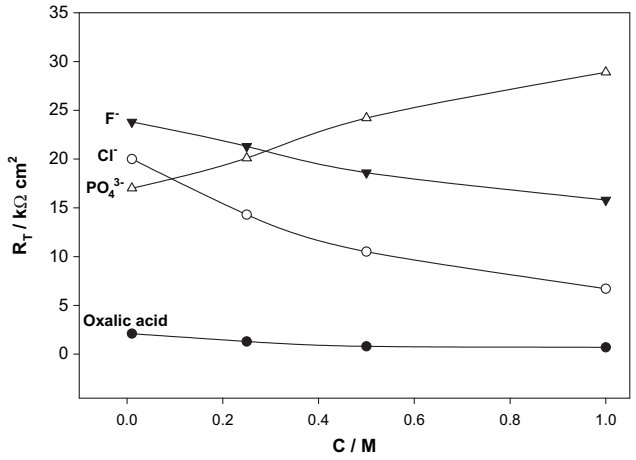

Fig. 6 – Variation of R_T of AZ31E electrode as a function of concentration for oxalic acid and Cl^-, F^- or PO_4^{3-} anions in naturally aerated 0.01 M oxalic acid solution, at 298 K.

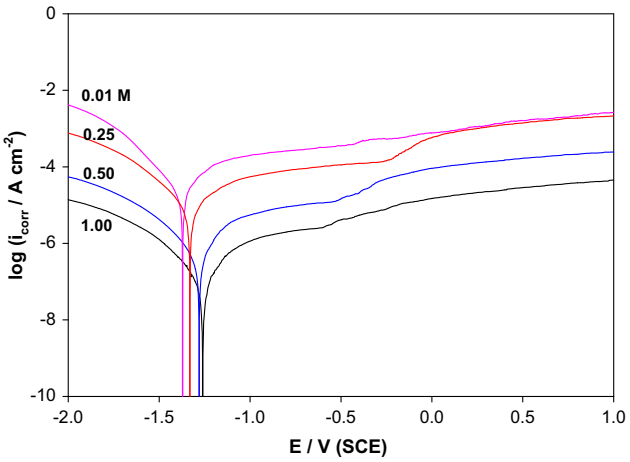

Fig. 8 – Potentiodynamic polarization scans of AZ31E electrode as a function of concentration for PO_4^{3-} anion in naturally aerated 0.01 M oxalic acid solution, at 298 K.

flower like structure was formed that is much better than the blank. On adding 0.01 M of F^- to the blank (Fig. 7c), the grain particles of the salt film grow laterally [8] during the prolonged exposure (for 2 h) covering nearly the whole surface of the alloy indicating more stability as compared to the blank. Finally, Fig. 7d is for 0.01 M Cl^- ion added to the blank, which contains a film on the surface like beehive structure.

3.3. *Potentiodynamic polarization measurements*

The Potentiodynamic polarization behavior of the AZ31E electrode was studied in relation to concentration of oxalic acid electrolyte. Fig. 8 shows a linear sweep potentiodynamic traces for the tested electrode in 0.01 M oxalic acid solution with different concentrations (0.01–1.0 M) of PO_4^{3-} ion, at a scan rate of 1 mV/s over the potential range from −2.0 to 1.0 V vs. SCE. Prior to the potential sweep, the electrode was left under open circuit in the respective solution for 2 h until a steady state free corrosion potential was reached. Obviously, increasing the concentration of oxalic acid increases the corrosion current density as shown in Fig. 9. This may reflect the changing of the nature of the film formed on the surface (may represent the replacement of MgO by $Mg_2C_2O_4$).

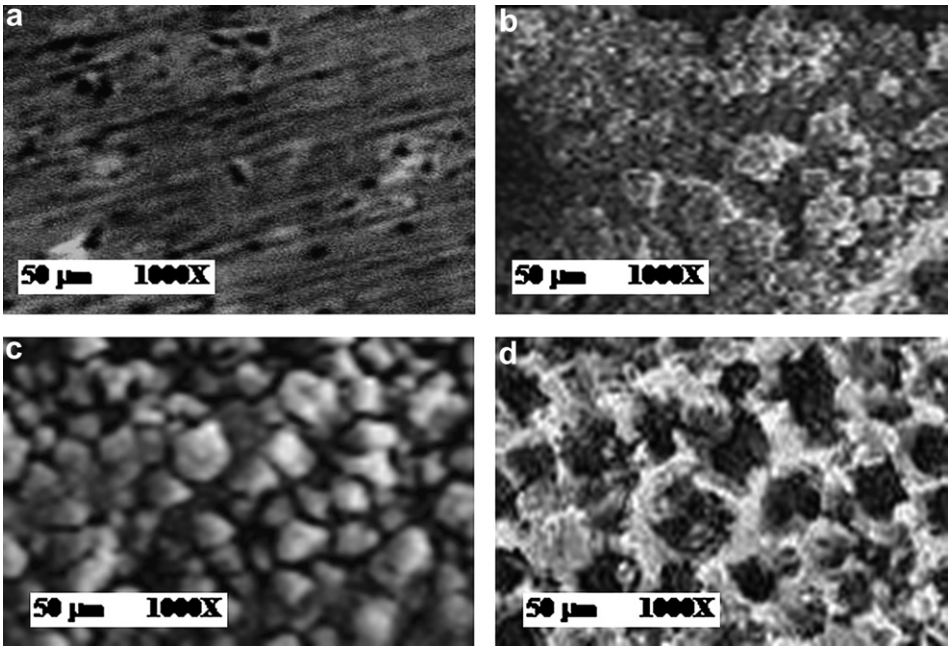

Fig. 7 – SEM micrographs of AZ31E electrode in naturally aerated a) 0.01 M oxalic acid solution (blank) containing b) Cl^-; c) F^- or d) PO_4^{3-} anions (0.01 M), at 298 K.

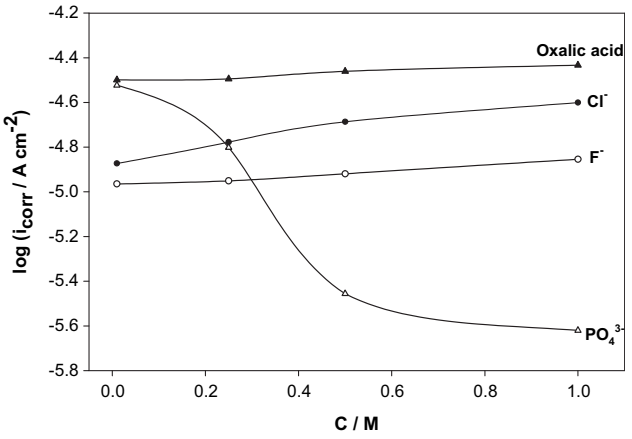

Fig. 9 – Variation of the logarithm of corrosion current density (i_{corr}) for AZ31E electrode as a function of concentration for oxalic acid and Cl^-, F^- or PO_4^{3-} anions in naturally aerated 0.01 M oxalic acid solution, at 298 K.

The effect of added Cl^- or F^- or PO_4^{3-} ions on the electrochemical behavior of the tested AZ31E electrode in 0.01 M $H_2C_2O_4$ solution at 298 K is shown in Fig. 9. It was found that i_{corr} value increases with increasing either Cl^- or F^- ion concentration reflecting the harmful effect of chloride or flouride ions leading to an increase in hydrogen evolution [2,13] and corrosion rate. For phosphate ion, increasing its concentration leads to a decrease in i_{corr} value which means that the corrosion rate decreases. So, phosphate is useful in reducing the corrosion or hydrogen evolution rate [14,15]. These results coincide with that drawn from OCP and EIS data.

Based on these facts, the overall reaction of AZ31E can be described as [7]:

- *Anodic reactions*

$$Mg + 2OH^- = Mg(OH)_2 + 2e \text{ (alkaline solution)} \quad (5a)$$

also,

$$\left.\begin{array}{c} Mg = Mg^{2+} + 2e \\ Mg^{2+} + H_2O = MgO + 2H^+ \\ Al = Al^{3+} + 3e \end{array}\right\} \text{(acid solution)} \quad (5b)$$

- *Cathodic reactions*

$$2H_2O + 2e = 2OH^- + H_2\uparrow \text{(alkaline solution)} \quad (6a)$$

$$2H^+ + 2e = H_2\uparrow \text{ (acid solution)} \quad (6b)$$

due to the immense reactivity of AZ31E alloy in acid medium, hydrogen is also produced directly through the following reaction:

- *Chemical reaction*

$$2Mg + 2H^+ + 2H_2O = 2Mg^{2+} + 2OH^- + 2H_2\uparrow \quad (7)$$

The equilibrium pH value required for the precipitation of $Mg(OH)_2$ is around 11.0, which means that 0.01 M oxalic acid containing phosphate ions (pH 11.1) are in favor of direct precipitation of $Mg(OH)_2$ better than the other two anions fluoride or chloride in acidic solution (0.01 M oxalic acid solution). Therefore, decrease in solution pH increases the corrosion kinetics and the alloy degradation proceeds with a much higher rate.

Generally, for comparing corrosion rate obtained from Tafel and EIS measurements, it is well known that the polarization resistance R_p is related to the corrosion rate through Tafel slopes β_a and β_c by Stern–Geary equation [16]:

$$i_{corr} = \frac{1}{2.303R_p\left(\frac{1}{\beta_a} + \frac{1}{|\beta_c|}\right)} \quad (8)$$

Table 4 – Corrosion rate (P_i) calculated from EIS and Tafel methods of AZ31E electrode as a function of concentration for Cl^-, F^- and PO_4^{3-} anions in naturally aerated 0.01 M oxalic acid, at 298 K.

Anion	C	R_T	$i_{corr(EIS)}$	$P_{i(EIS)}$	$i_{corr\ (Tafel)}$	R_p	$P_{i(Tafel)}$
	M	KΩ cm^2	μA cm^{-2}	mm/y	μA cm^{-2}	kΩ cm^2	mm/y
Cl^-	blank	2.10	109.4	2.50	31.7	7.24	0.72
	0.01	20.0	14.28	0.33	13.4	21.3	0.31
	0.25	14.3	19.41	0.45	16.7	16.7	0.38
	0.50	10.5	26.16	0.59	20.6	13.4	0.47
	1.00	6.70	41.1	0.93	25.1	10.9	0.57
F^-	blank	2.10	109.43	2.50	31.7	7.24	0.72
	0.01	23.8	18.93	0.43	10.8	41.5	0.25
	0.25	21.3	21.44	0.49	11.2	40.8	0.26
	0.50	18.6	25.57	0.58	12.1	39.5	0.28
	1.00	15.8	27.07	0.62	14.0	30.6	0.32
PO_4^{3-}	blank	2.10	109.43	2.50	31.7	7.24	0.72
	0.01	17.0	41.98	0.96	30.0	23.8	0.69
	0.25	20.1	32.36	0.74	15.8	41.2	0.36
	0.50	24.2	8.391	0.19	3.50	58.1	0.08
	1.00	28.9	5.883	0.13	2.41	70.8	0.06

As given in Table 4, it can be seen that evaluated R_p values obtained from Tafel measurements have the same trend as R_T obtained from EIS measurements. By calculating i_{corr} from EIS measurements using cathodic, anodic slopes and R_T, it was found that they also have the same trend as that obtained from Tafel measurements. By calculation of corrosion rate, where i_{corr} (mA cm^{-2}) is related to the average corrosion rate in mm/y (P_i) using [4]:

$$P_i = 22.85\ i_{corr} \quad (9)$$

It was found that corrosion rate obtained from EIS method is comparable with that obtained from Tafel extrapolation method. Thus there is a good agreement between corrosion rates determined by both techniques.

4. Conclusions

- The corrosion rate of AZ31E magnesium alloy in oxalic acid solution depends on the concentration of the solution and the additive. A concentrated oxalic acid solution with lowest pH and highest hydrogen evolution is the more corrosive one.
- Oxalic acid solution of 0.01 M concentration containing Cl^- or F^- are more corrosive with increasing their concentrations from 0.01 to 1.0 M as observed from OCP, impedance or polarization techniques.
- For PO_4^{3-} anion in 0.01 M oxalic acid solution, it acts passivator. The corrosion rate decreases with increasing its concentration.
- All results were confirmed with SEM images.

REFERENCES

[1] Heakal FE, Fekry AM, Fatayerji MZ. Electrochemical behavior of AZ91D magnesium alloy in phosphate medium–part I. J Appl Electrochem 2009;39:583.

[2] Uan JY, Cho CY, Liu KT. Generation of hydrogen from magnesium alloy scraps catalyzed by platinum-coated titanium net in NaCl aqueous solution. Int J Hydrogen Energy 2007;32:2337.

[3] Fekry AM, El-Sherief R. Electrochemical corrosion behavior of magnesium and titanium alloys in simulated body fluid. Electrochim Acta 2009;54:7280.

[4] Ghoneim AA, Fekry AM, Ameer MA. Electrochemical behavior of magnesium alloys as biodegradable materials in Hank's solution. Electrochim Acta 2010;55:6028.

[5] Fekry AM. The influence of chloride and sulphate ions on the corrosion behavior of Ti and Ti-6Al-4V alloy in oxalic acid. Electrochim Acta 2009;54:3480.

[6] Maruthamuthu P, Ashokkumar M. Hydrogen generation using Cu(II)/WO_3 and oxalic acid by visible light. Int J Hydrogen Energy 1988;13:677.

[7] Heakal FE, Fekry AM, Fatayerji MZ. Influence of halides on the dissolution and passivation behavior of AZ91D magnesium alloy in aqueous solutions. Electrochim Acta 2009;54:1545.

[8] Fekry AM, Fatayerji MZ. Electrochemical corrosion behavior of AZ91D alloy in ethylene glycol. Electrochim Acta 2009;54:6522.

[9] Jain AK, Acharya NK, Kulshreshtha V, Awasthi K, Singh M, Vijay YK. Study of hydrogen transport through porous aluminum and composite membranes. Int J Hydrogen Energy 2008;33:346.

[10] Ma LP, Wang P, Cheng HM. Hydrogen sorption kinetics of MgH_2 catalyzed with titanium compounds. Int J Hydrogen Energy 2010;35:3046.

[11] Heakal FE, Fekry AM, Fatayerji MZ. Electrochemical behavior of AZ91D magnesium alloy in phosphate medium–Part II. Induced passivation. J Appl Electrochem 2009;39:1633.

[12] Muñoz LD, Bergel A, Féron D, Basséguy R. Hydrogen production by electrolysis of a phosphate solution on a stainless steel cathode. Int J Hydrogen Energy 2010;35:8561.

[13] Ameer MA, Fekry AM. Inhibition effect of newly synthesized heterocyclic organic molecules on corrosion of steel in alkaline medium containing chloride. Int J Hydrogen Energy 2010;35(20):11387–96.

[14] Fekry AM, Ameer MA. Corrosion inhibition of mild steel in acidic media using newly synthesized heterocyclic organic molecules. Int J Hydrogen Energy 2010;34:7641.

[15] Azizi O, Jafarian M, Gobal F, Heli H, Mahjani MG. The investigation of the kinetics and mechanism of hydrogen evolution reaction on tin. Int J Hydrogen Energy 2007;32:1755.

[16] Boudjemaa A, Boumaza S, Trari M, Bouarab R, Bouguelia A. Physical and photo-electrochemical characterizations of α-Fe_2O_3. Application for hydrogen production. Int J Hydrogen Energy 2009;34:4268.